JOURNAL OF GEOPHYSICAL RESEARCH, VOL. 92, NO. C11, PAGES 11,709–11,726, OCTOBER 15, 1987

Five-Year Climatological Survey of the Gulf Stream System and Its Associated Rings

STEPHEN J. AUER[1]

Ocean Products Center, National Meteorological Center, Camp Springs, Maryland

A 5-year climatological survey of the Gulf Stream System's landward surface edge defines the mean, standard deviation, extreme limits, annual and interannual variabilities, and frequency distributions along 0.5° longitudinal transects from 91° to 44°W. The climatology covers the Loop Current in the Gulf of Mexico and the Gulf Stream in the northwest Atlantic Ocean. Autocorrelations and power spectra are derived for longitudinal transects between 79.5° and 57.5°W. The study also investigates the observed warm-core ring and cold-core ring movements and their areal extent. The observed data are compiled from the Oceanographic Analysis charts (produced by the National Oceanic and Atmospheric Administration) which utilize infrared satellite imagery and in situ observations. East of Cape Hatteras the Gulf Stream System Landward Surface Edge exhibits both interannual and annual signals. The interannual variability is equal to the annual variability. The mean monthly Gulf Stream position for the longitudinal band 70°–44°W shifts from farthest north in September to farthest south in February. The magnitude of the annual shift is largest near the Grand Banks. Frequency distributions of the Gulf Stream System position are quasi-normal nearly everywhere. Autocorrelation plots from the 5-year time series of Gulf Stream positions at longitudinal transects 79.5°–57.5°W exhibit three well-defined *e*-folding time regimes with a maximum time of 10 weeks at 72°W. Power spectrums from 79.5° to 57.5°W are red spectrums having dominant peaks of 1-year period or greater. The largest total spectra energies are found at 61°W. The Loop Current sheds rings at two apparent spatial scales which are labeled major (307-km mean) and minor (185-km mean) warm-core rings. Annually, the Loop Current sheds about one major warm-core ring which translates into the western basin of the Gulf of Mexico and one minor warm-core ring which is usually reabsorbed by the Loop Current. The major Loop Current warm-core ring sheddings have no seasonal preference. Loop Current warm-core rings have a mean velocity of 2.4 km/d west-southwest. An average of 22 Gulf Stream warm-core rings are formed and absorbed annually between 75° and 44°W. The largest frequency of warm-core ring formations is seen near the New England Seamounts, while the largest frequency of warm-core ring absorptions is found near Cape Hatteras. Gulf Stream warm-core rings can absorb each other as occurred in 14% of the absorption cases with the highest frequency just upstream of the New England Seamounts. The Gulf Stream warm-core rings have a surface diameter decay rate of −0.026 per week (Loop Current warm-core rings are similar). The Gulf Stream warm-core rings have a mean velocity of 2.4 km/d west-southwest. Cold-core rings have a mean cool-core surface diameter of 105 km and a mean velocity of 1 km/d southwest. More definitive conclusions on cold-core rings are not possible, as ring identification and tracking by satellite infrared imagery is tentative.

1. INTRODUCTION

The Gulf Stream System, the best known of the western boundary currents, can be arbitrarily subdivided into two major sections: (1) the Loop Current located in the Gulf of Mexico and (2) the Gulf Stream located in the northwest Atlantic Ocean. The Loop Current enters the Gulf of Mexico from the Caribbean Sea via the Yucatan Strait and penetrates a variable distance northward into the Gulf of Mexico before exiting via the Florida Straits. The Loop Current periodically pinches off, forming large warm-core rings which tend to drift westward into the western basin of the gulf [*Cochrane*, 1972]. The Gulf Stream continues downstream of the Loop Current flowing into the northwest Atlantic Ocean from the Florida Straits and then flowing northward just seaward of the continental shelf break along the southeast United States as far north as Cape Hatteras. The Gulf Stream then departs from the shelf break and flows northeastward past the Grand Banks.

The Loop Current has a mean volume transport of about 30 Sv (Sv = 10^6 m^2 s^{-1}) [*Nowlin*, 1972]. The mean transport of the Gulf Stream is 30 Sv near Miami, Florida [*Niiler and Richardson*, 1973], increases to 85 Sv near Cape Hatteras [*Worthington and Kawai*, 1972] as a result of input from the southward gyre recirculation and cold-core ring absorptions, further increases to 150 Sv near 65°W [*Worthington*, 1976], and apparently thereafter decreases to about 110 Sv near the Tail of the Grand Banks [*Worthington*, 1976] due to ring formations and the southward gyre recirculation.

Past Cape Hatteras the Gulf Stream often exhibits large meanders which occasionally pinch off, forming warm-core rings or, alternatively, cold-core rings [*Hansen*, 1970]. These rings are an important factor in the recirculation of the Gulf Stream and in the chemical and biological makeup of the slope water north of the stream and the Sargasso water south of the stream [*Ring Group*, 1981].

This report is significant in defining a climatology which encompasses the Loop Current, the Gulf Stream, and their associated ring events and movements over a relatively long, continuous 5-year period using the same data base. The first "climatological" charts of the Gulf Stream are attributed to Folger or Ben Franklin [*Richardson*, 1980*a*]; other generalized reports followed. A problem intrinsic to all these early descriptions is the difficulty of defining the current boundaries from point observations scattered in space and time (that is, no large-scale synoptic observations). Several ship and plane

[1]Now at National Environmental Satellite, Data, and Information Service, Suitland, Maryland.

Paper number 7C0602.

surveys of the recent past, such as *Fuglister and Worthington* [1951] and *Robinson et al.* [1974], adequately mapped sections of the stream in one-dimensional horizontal tracks, but these did not cover all the stream and had large temporal gaps between surveys. The advent of remote sensing on satellite platforms has provided an inexpensive and relatively accurate two-dimensional large-scale horizontal detection of the Gulf Stream System. Recently, subsurface moored arrays of inverted echo sounders have successfully demonstrated their ability to accurately and continuously monitor the stream's path over a limited region [*Watts and Johns*, 1982; *Tracey and Watts*, 1986].

The observations used in this study are predominantly derived from infrared Advanced Very High Resolution Radiometer polar-orbiting satellite imagery which can resolve the sea surface temperature (SST) within 0.5°C [*McClain et al.*, 1985] and performs even better in resolving SST gradients. *Vazquez and Watts* [1985] estimate that the stream position measurement error near Cape Hatteras from satellite imagery is ± 10 km, about the resolution of the imagery. This measurement error value increases downstream to an estimated ± 30 km in the Newfoundland Basin where there are fewer land reference points for registering the imagery. *Fuglister and Voorhis* [1965] and *Hansen and Maul* [1970] both found the maximum surface temperature gradient front of the Gulf Stream (subjectively discerned from satellite imagery) to be about 15 km landward of the classical in situ definition (15°C at 200 m depth) of Fuglister and Voorhis. *Olson et al.* [1983] also found the satellite-derived Gulf Stream surface front to agree well with in situ data.

The term Gulf Stream Landward Surface Edge (GSLSE) is utilized in this paper to denote the current's edge nearest to the North American continental landmass. This same edge in the northwest Atlantic Ocean is synonymously referred to as the "north wall" or "cold wall" [*Stommel*, 1960] of the Gulf Stream due to the large temperature gradient inherent across it.

The study findings and discussions will be presented in this sequence. First, the data source and the analysis methods will be given as a background for revealing the results. Then, the results will be presented and discussed in four separate groupings beginning with the 5-year GSLSE statistics. Next, the Gulf Stream System's associated rings will be presented in three groups, the Gulf Stream warm-core rings (GS WCRs), the Loop Current warm-core rings (LC WCRs), and the cold-core rings (CCRs). Finally, the conclusion will attempt to link the separate discussions into a broad cohesive statement of the study findings.

2. Data Source

The 5-year weekly data set contains an Eulerian representation of the weekly GSLSE positions and a Lagrangian description of the center positions and average diameters of the WCRs and the CCRs. The data set was manually compiled from 1300 Oceanographic Analysis Charts, hereafter referred to as "charts." The charts are produced by the National Weather Service and the National Environmental Satellite, Data, and Information Service. The charts contain positions of ocean thermal fronts which are manually analyzed from polar-orbiting satellite infrared imagery along with available expendable bathythermograph reports and data buoy and ship SST observations [*Auer*, 1980; *Gemmill and Auer*, 1982]. The advantages of using the charts as a data source are the frequency of analysis (thrice weekly north of Cape Hatteras and twice weekly south of Cape Hatteras), the large continuous region of coverage, the long period of coverage (over 5 years), the high resolution (1 km) of the infrared satellite imagery, and the quality and continuity of the manual analysis (most of the charts were analyzed by the same experienced, principal satellite imagery analyst during the 5 years). One drawback in using the charts is the occasional long data gaps in some regions due to persistent cloudiness and the annual relaxation of the temperature gradient which conceal frontal boundaries.

The five daily charts were assimilated into one digital weekly analysis by preferentially time centering the observed feature positions about midnight Thursday. The GSLSE latitudinal position to the nearest 0.1° was determined at each 0.5° longitudinal transect from 91.0° to 44.0°W. The weekly WCR and CCR observations were compiled with a ring name, a center position, and an average diameter. Ring formation and absorption events were also noted. When possible, the ring names are the same names as found in the *Oceanographic Monthly Summary* (published by NOAA since 1981) or its predecessor, the *gulfstream* (published by the National Weather Service through 1980). In some instances the ring names or movements reported in the above-mentioned publications were corrected during the extensive review of all the charts. These ring corrections are an acceptable result of the advantage of more accurately determining the ring events after the complete history of observed ring movements is known, a luxury not available to the real time schedule of the monthly publications.

After its initial compilation the 5-year weekly data set was carefully scrutinized by several manual and objective quality control/error checking procedures. In spite of these efforts the final data set presented in this report may inadvertently still contain a few errors due to the subjective nature of the tasks involved in the original analysis and registration of the (satellite imagery) data and the later data set compilation (digitization of the charts). An estimate of the GSLSE error is found in the work by *Vazques and Watts* [1985], who compared the Gulf Stream path just downstream from Cape Hatteras between 30 satellite images processed by Peter Cornillon of the University of Rhode Island and their digitized chart positions and calculated an rms difference of ± 20 km. The GSLSE position error may in fact be larger farther downstream from Cape Hatteras due to the sparsity of land points available to geographically align the satellite imagery. *Brown et al.* [1986] determined an rms error of ± 15 km in latitude and longitude between four Gulf Stream warm-core ring center chart positions and a precision analysis of digital satellite imagery by researchers at the Universities of Miami and Rhode Island. The most reliable and representative climatological GSLSE positions and ring statistics should exist in areas and during periods where they were most frequently observed (see Figure 2). The first year's GSLSE weekly observations have been previously summarized [*Auer*, 1983].

3. Analysis Method

The gross statistics (mean, standard deviation, extremes) of the 5-year weekly data set are computed for each 0.5° longitudinal transect at 5-year, yearly, and seasonal time frames. Table 1 lists the beginning and ending dates for years 1–5.

TABLE 1. Weekly End Point Dates for Years 1–5

Year	Begin Week	End Week
1	May 30, 1980	May 20, 1981
2	May 27, 1981	May 19, 1982
3	May 26, 1982	May 18, 1983
4	May 25, 1983	May 17, 1984
5	May 24, 1984	May 16, 1985

Two crossing points (northern and southern) are needed to define the GSLSE in the western Loop Current (91°–86.5°W) and along the Florida east coast at 80°W. At other longitudes for the occasional weekly multivalued stream crossings the northernmost weekly crossing is used in determining the mean, standard deviation, and northern extreme crossing; the southernmost weekly crossing is used in determining the southern extreme crossing. One drawback and an important consideration to be borne in mind when analyzing the computed statistical positions is the relative orientation of the mean GSLSE path to the longitudinal transects. Where the relationship is nonorthogonal, the standard deviation and the ranges will tend to to be overestimated, but the mean and extreme positions will be unaffected. The impact of the nonorthogonality is addressed later in this paper.

The study determines the latitudinal frequency distribution of the GSLSE at each longitudinal transect.

Individual sets of 5-year time series are created for the GSLSE crossings between 79.5° and 57.5°W, where the GSLSE observation frequencies (Figure 3) are greater than 75%. Data gaps within the time series are filled in by linearly interpolating the missing weekly positions. Normalized temporal autocorrelations, e-folding times, and power spectra are then determined for these time series.

The weekly WCR and CCR observations are stratified by ring name, forming a chronological track of each ring's movements. The ring movements between the weekly (or longer) observations are determined by the ring's center position change. If the ring's formation date and size are known, then a ring age (weeks) and (observed/initial) diameter ratio are determined for each subsequent observation; these are later used to calculate the ring diameter decay rate. The gross statistics of (scalar) speed, velocity, lifetime, and translation are then computed for ring type, geographical region, year, and season.

4. Gulf Stream Landward Surface Edge

4.1. *Climatological Statistics*

Figure 1 shows all the observed weekly GSLSE positions during the 260-week (5-year) data period; it illustrates the northward (and slightly westward) intrusive nature of the Loop Current, the expanding range of the GSLSE downstream from Cape Hatteras, and the increased meandering downstream from Cape Hatteras [*Hansen*, 1970].

Figure 2, which gives the 5-year and the seasonal percentages of GSLSE observations at nine selected longitudinal transects, reveals geographical and seasonal differences for GSLSE observations. The Gulf of Mexico GSLSE (Loop Current) is only observed for 60% of the weeks. This percentage rises to 85% at 80°W, remains above 85% downstream to 60°W, and steadily decreases to about 40% at 45°W. Most of the missing weekly observations are due to the blockage and contamination of the SST radiation to the satellite radiometer by persistent cloudiness. Generally, summer and winter exhibit the seasonal frequency extremes. Winter has the highest seasonal frequency upstream of Cape Hatteras but the lowest frequency downstream of Cape Hatteras. Summer Loop Current observations are rare, as the intense insolation weakens or erases the SST gradient signal of the GSLSE. This condition lasts from about June 22 to October 25 (5-year average). Interestingly, *Auer* [1982] reports that the Loop Current may occasionally be discerned by the SST signal in late July or August when the sign of the SST gradient reverses as the Caribbean water advected by the loop is slightly cooler than the surrounding gulf water. This phenomenon is evident

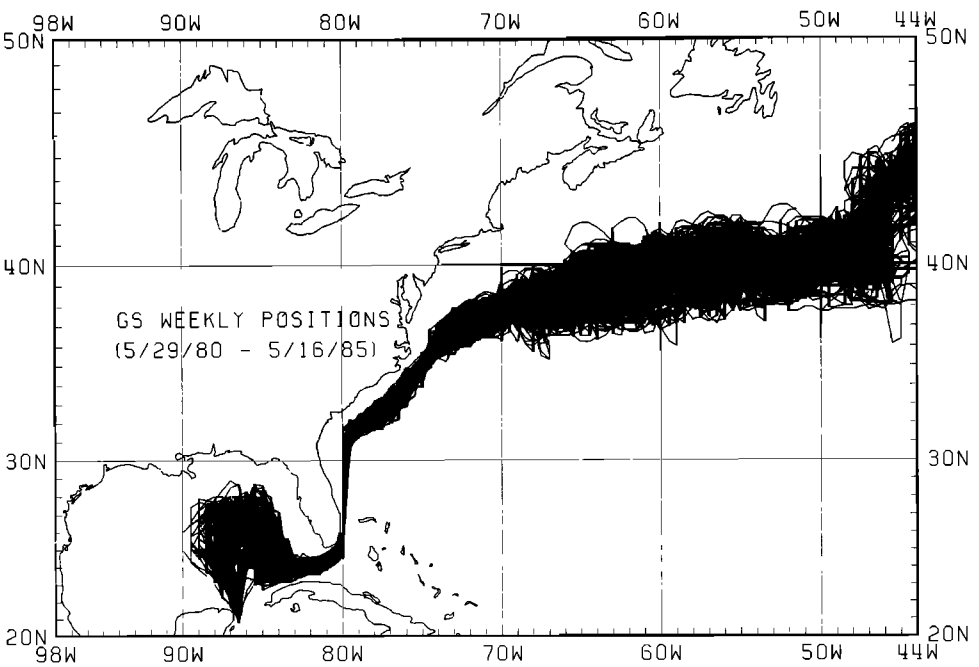

Fig. 1. The observed weekly Gulf Stream System Landward Surface Edge positions for 260 weeks (5-year data period).

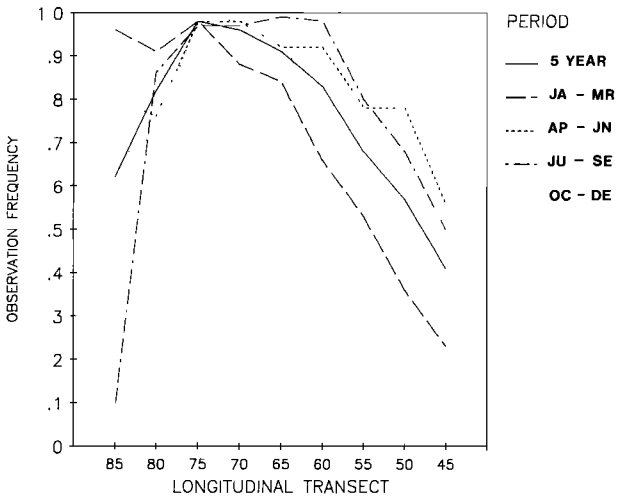

Fig. 2. The 5-year and seasonal percentages of Gulf Stream Landward Surface Edge observations at nine selected longitudinal transects. The edge is most frequently observed near Cape Hatteras (75°W). Winter observations near the Grand Banks (45°W) and summer observations in the Gulf of Mexico (85°W) are infrequent.

in both satellite imagery (in 1982 and 1986) and the climatological SST record [*Robinson et al.*, 1979].

Table 2 contains the 5-year record of Loop Current observations for each transect from 90.5° to 86°W. The second column gives the number of weeks of good data. The third and fourth columns stratify the good data weeks by the presence or absence of the Loop Current. Table 2 provides the basis for arbitrarily determining the mean western extension of the Loop Current to be at 88.0°W, where the loop is present over 50% of the time. The percentages are dramatically different for the adjacent transects to the west (24% for 88.5°W) and east (74% for 87.5°W). This percentage decline near 88°W is consistent in each of the 5 years. Thus the loop shows little interannual variability (<0.5° longitude) along its western edge.

Figure 3 presents the 5-year climatological GSLSE curves. None of these curves is representative of any particular week's synoptic GSLSE position.

The extreme GSLSE curves connect the most northern (and southern) observed positions between the transects. The extreme curves reveal the expansive intrusion range of the Loop Current to the north and west. The GSLSE range at 86.5°W (a good reference longitude for monitoring Loop Current penetration) is 8.2° of latitude. The northernmost observed extreme of the loop is 29.1°N at 87°W; this is less than the extreme excursions to 30°N reported at the surface by *Huh et al.* [1981] and *Vukovich et al.* [1979] or to 29.5°N in subsurface hydrographic data presented by *Sturges and Evans* [1983]. The range narrows in the Florida Straits, then slightly widens along the Carolinas (75°–80°W) where small-amplitude wave-like meanders often propagate downstream with a prominent weekly time scale [*Webster*, 1961]. Accordingly, past Cape Hatteras, large-amplitude meanders are observed to grow, translate, and occasionally pinch off or reform. The GSLSE range increases downstream from 75°W to a local maximum near 65°W. This study did not find the existence of a local range minimum near 70°W reported by *Cornillon* [1986], but it did confirm the significant range increase near 69°W. Past 65°W the GSLSE range is stable and then slowly decreases to a local minimum near 50°W. The GSLSE range increases significantly near 48°W. The largest GSLSE range is 9.9° of latitude at 45°W.

TABLE 2. Loop Current Western Edge Variability

Longitude	Number of Weeks Data Available	Number of Weeks Loop Absent	Number of Weeks Loop Present	Percent of Time Loop Present
90.5°W	156	156	0	0%
90.0°W	156	155	1	1%
89.5°W	158	149	9	6%
89.0°W	160	137	23	14%
88.5°W	161	122	39	24%
88.0°W	161	68	93	58%
87.5°W	162	42	120	74%
87.0°W	167	27	140	84%
86.5°W	164	3	161	98%
86.0°W	159	0	159	100%

The mean GLSE curve for the Loop Current has an arbitrary straight-line western edge along 88°W (discussed previously in reference to Table 2). The mean Loop Current curve compares well (±0.5°) with the *Baig et al.* [1981] 4-year mean loop position derived from lower-resolution satellite imagery. The small indentation of the mean loop at 86.5°W is a result of the variation in the Loop Current's penetration due to major Loop Current warm-core ring shedding events.

The straight-line section of the mean GSLSE running north along 80°W is poorly resolved by two widely spaced (mean southward and northward crossing) points. The best climatology along 80°W is found in a 5-year study of the weekly U.S. Navy Ocean Frontal Analysis (a satellite analysis) by *Olson et al.* [1983] which determined statistical positions normal to the mean stream path. The Olson study shows the GSLSE mean path to be slightly east of 80°W (about 20 km) from 26° to 28°N and slightly west of 80°W from 29° to 30°N.

The mean GSLSE curve exhibits a seaward deflection of the stream near 32°N 78°W which is, at least partly, the result of bottom steering by the Charleston Bump bathymetric feature [*Legeckis*, 1979; *Bane*, 1982]. The mean GSLSE positions from 80° to 75°W agree with the 5-year mean surface path of *Olson et al.* [1983].

The mean curve smooths out all the large synoptic meanders east of 70°W as seen in the daily charts. The mean GSLSE curve from 74° to 58°W agrees with the 3-year (1979–1981) mean of *Vazquez and Watts* [1985] and the 2.5-year (1982–1984) mean of *Cornillon* [1986] which are both derived from satellite imagery. The mean GSLSE path direction is east-northeast from 75° to 48°W. The mean GSLSE path between 65° and 60°W is nearly straight and shows scant evidence of *Richardson*'s [1981] quasi-permanent 100-km southeastward deflection of the stream over the New England Seamount chain as detected by 35 remotely tracked surface drifters. The two crests near 50°W and 56°W and the intermediate trough near 53.5°W are barely significant (95% confidence level) features in the mean climatological curve. These questionable bump features, if not artifacts of the GSLSE data set, would indicate the more frequent presence of meanders.

The Gulf Stream flow in the area past 50°W is controversial. *Worthington* [1976] suggests a two-gyre system with the Gulf Stream recirculating southward, but *Dietrich et al.* [1975] counters that a bifurcation of the Gulf Stream occurs east of this area into the North Atlantic Current and the

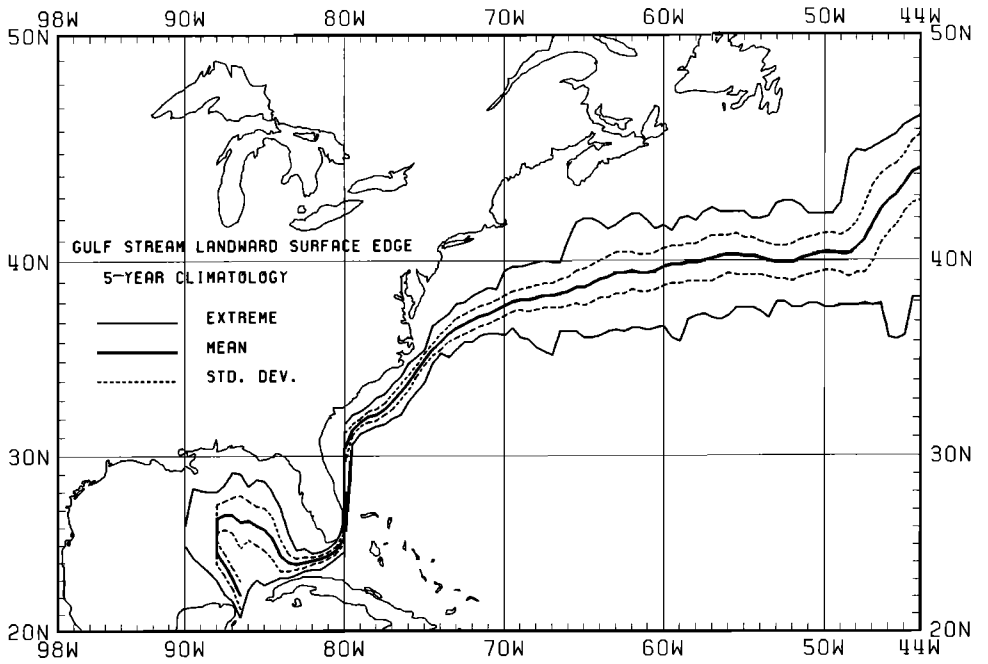

Fig. 3. The 5-year climatological curves of the Gulf Stream System Landward Surface Edge defined for each 0.5° of longitude. The bold solid line delineates the mean position. The dashed lines delineate a one standard deviation envelope about the mean. The light solid lines delineate the 5-year observed extreme excursions.

southward recirculation. The surface pattern of the mean GSLSE appears to agree with Dietrich showing a northward flow into the North Atlantic Current. The abrupt shift of the mean GSLSE path past 48°W to the northeast is perhaps due to the stream's departure from the constraining influences of both the Labrador Current and the Grand Banks topographic feature.

The aliasing of the short-period variance (less than 2 weeks) is probably not substantial for much of the GSLSE, except possibly in the region 80°–70°W. The nonorthogonality of the 0.5° longitudinal transects to the mean GSLSE path is a larger concern. The variability from 80° to 73°W is overestimated as a result, except at 78.5°–78.0°W. Fortunately, other studies have covered this area quite well [*Vazquez and Watts*, 1985; *Halliwell and Mooers*, 1983; *Olson et al.*, 1983] with orthogonally oriented synoptic measurements. For the Loop Current

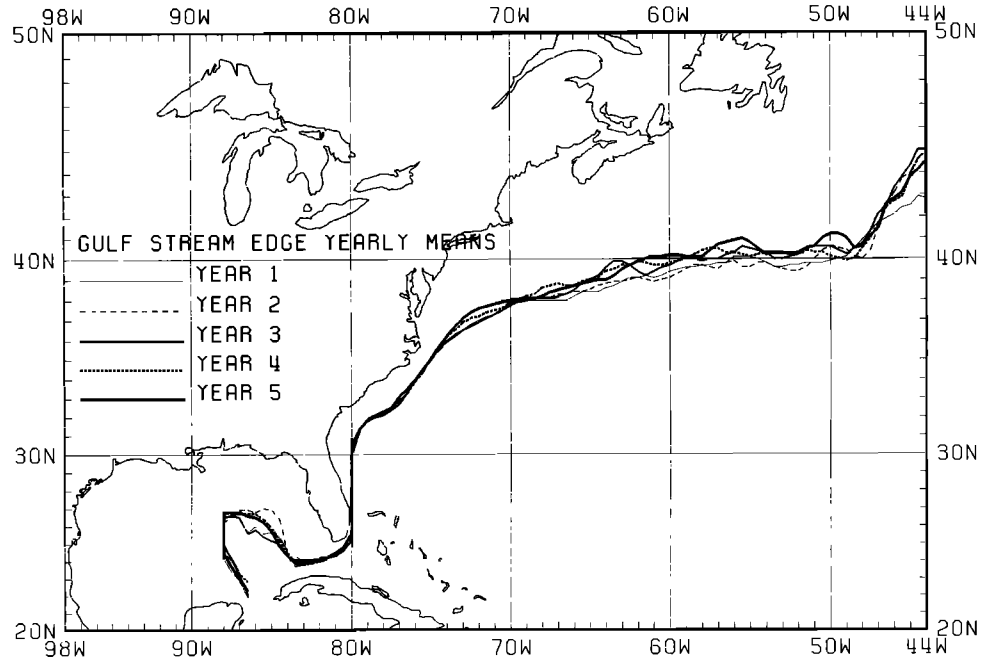

Fig. 4. Comparison of the Gulf Stream Landward Surface Edge yearly mean curves. The year dates are given in Table 1. Interannual variability is seen in the Loop Current's northward penetration at 86.5°W and in the Gulf Stream north of Cape Hatteras.

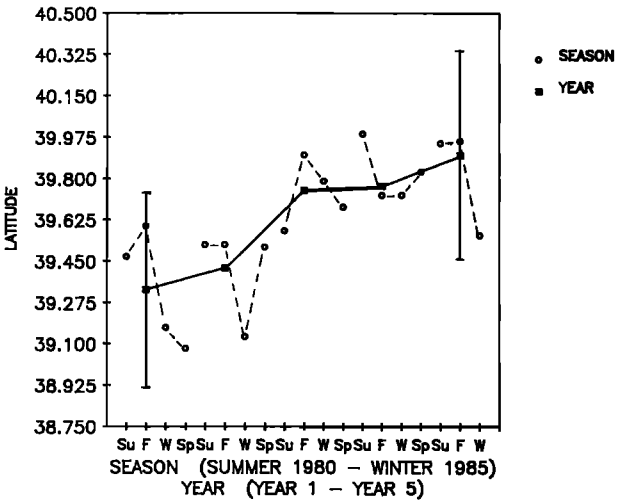

Fig. 5. The 5 yearly and 19 seasonal mean Gulf Stream Landward Surface Edge positions over the longitude band 74°–44°W. Confidence limits (95%) are drawn for years 1 and 5. An incremental northward shift is seen over years 1–5. Year 1 is found to be significantly south of year 5. An F test of these two samples indicates that the interannual variability is equal to the annual variability.

and for the Gulf Stream downstream of 70°W this study's stream variability results are probably the best to date because of the long record of frequent measurements.

The GSLSE's 165-km standard deviation at 86.5°W indicates the loop's large penetration variability. The standard deviation is smallest (20 km) in the Florida Straits. The large standard deviation seen at the 80°W north crossing should be discarded due to the extreme nonorthogonality of the transect to the mean path. *Olson et al.* [1983] calculated GSLSE standard deviations from 26° to 30°N (these run roughly along 80°W) to be less than 20 km, indicating small meridional variability.

The standard deviations along the Carolinas are nearly constant at about 35 km, but they are larger than the 5–10 km measurements of *Olson et al.* [1983]. The standard deviations increase and remain nearly constant at about 55 km from just east of Cape Hatteras to 69°W, then increase to 100 km near 65°W. The values from 74.5° to 67.5°W are larger than the 10–20 km determined by *Vazques and Watts* [1985]. At 65°W the standard deviation value of 95 km compares reasonably well with the 80 km value of *Halliwell and Mooers* [1983]. The standard deviations remain nearly constant at 100 km from 65° to 48°W, rapidly double to a peak value of 200 km at 47°W and then decrease somewhat to 155 km at 44°W. The standard deviation jump near 47°W is probably a real feature resulting from the streams departure from the Grand Banks topographic feature; however, the magnitude of the standard deviation jump has some error associated with the nonorthogonality of the sampling to the mean path.

4.2. *GSLSE Annual and Interannual Varibility*

Figure 4 gives the five yearly mean GSLSE curves. Interannual variability is evident in the Loop Current's northward penetration, especially at 86.5°W, where years 2, 4, and 5 have a more northern position than years 1 and 3. This is caused by the Loop Current warm-core ring shedding variability (see Figure 17). The interannual variability is also evident in the stream east of Cape Hatteras. An examination of the charts and a time series plot (not shown) reveal that the GSLSE along 80°W shifted slightly eastward in year 5, as the northern crossing at 80°W moved southward from its normal position near 30°N to 26°N on several occasions.

Figure 5 gives the five yearly and 19 seasonal mean GSLSE latitude values for the longitudinal band 74°–44°W. Confidence limits are drawn for the means of years 1 and 5. A northward trend is seen in years 1–5. A one-tail student t test indicates that year 1 is significantly south of year 5. The reason for the northward trend of the GSLSE is unknown.

Figure 6 displays the seasonal mean GSLSE curves (summer curve unreliable as it represents only a few observations). The similar seasonal means for the Loop Current in Figure 6 imply that the Loop Current has no annual cycle as suggested by *Leipper* [1970] (fall curve does not show a yearly minimal Loop Current penetration, and the winter and spring curves do not show a Loop Current growth trend). Furthermore, Figure 17 indicates no seasonal bias for major LC WCR formations. *Behringer et al.* [1977] also suggested that the Loop Current has an annual cycle of spring growth and a single summertime eddy shedding event accompanied by Loop Current retreat. Nevertheless, Behringer et al. find much temporal variability between the (Loop growth and) eddy shedding events (8–17 months). *Sturges and Evans'* [1983] 13-year time series of Loop Current amplitude from hydrographic data displays a broad spectral peak with variations from 8 to 30 months.

An annual cycle is found (Figure 7) for the GSLSE in the longitudinal band 70°–44°W, where the March mean is significantly south of the September mean (65-km shift). Similar tests of an annual cycle in six smaller longitudinal bands over the region east of Cape Hatteras found no significant annual shift for bands 74°–70°W and 64.5°–60°W but found significant annual shifts for bands 69.5°–65°W (45 km), 59.5°–55°W (55 km), 54.5°–50°W (55 km), and 49.5°–44°W (175 km). The magnitude of the annual shift in the Grand Banks area is slightly inflated by the nonorthogonal transects; it may also have some error associated with cloud persistence which may bias wintertime observations to more southern crossings.

Other studies have also found this annual cycle. *Iselin* [1940] noted seasonal changes in the Gulf Stream transport near 68°W with a winter maximum (and accompanying axis shift to the south) and a fall minimum (axis shift to the north). Iselin also corroborated this with tide gauge records from Bermuda and U.S. east coast stations. *Fuglister* [1972] found that the stream's mean position from 75° to 50°W during 1965–1966 to be farther south in late winter when the oceanic heat loss was largest and farther north in the fall. For the region 71°–64°W, *Zheng et al.* [1984] found a 3-year average GSLSE southward shift of about 40 km from fall to winter (55 km from November to February). *Nof's* [1983] simplified two-layer model of a steady ocean current (Gulf Stream) forced by atmospheric cooling projects a southward deflection of about 45 km from the summer position to the winter position. This is consistent with the distance found in this study. In addition, Nof's Figure 8 hints that the GSLSE deflection may increase downstream, again consistent with this study.

Olson et al. [1983] found fall to winter southward deflections along the Carolinas near 33°N, which could not be confirmed by this study.

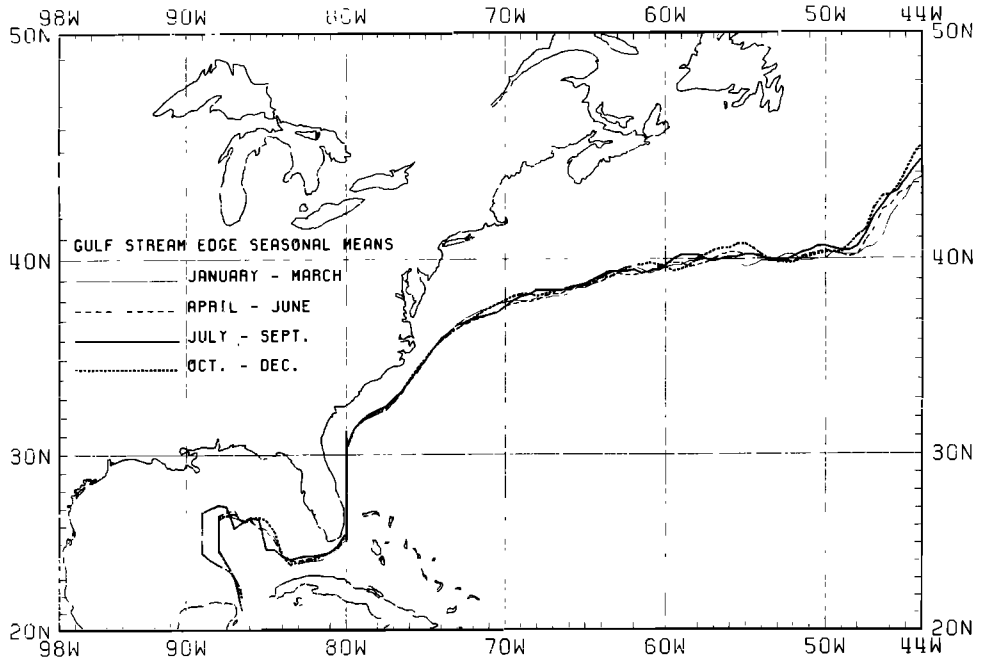

Fig. 6. Comparison of Gulf Stream Landward Surface Edge seasonal mean curves. An annual cycle is not found for the Loop Current (ignore the summer curve). An annual cycle is seen in some areas east of 70°W where the winter mean is in a more southern position than the fall and summer means.

The seasonal mean curves (Figure 6) exhibit less variability than the yearly mean curves (Figure 4) do, especially in the Loop Current (ignore the undersampled summer mean). An F distribution test of the five yearly and 19 seasonal mean samples (see Figure 5) for the region 74°–44°W indicates that the interannual variability is statistically similar to the annual variability.

4.3. *GSLSE Frequency Distribution*

Figures 8a-8d show the 5-year GSLSE frequency distributions observed at selected longitudinal transects. The frequency distribution for 86.5°W (Figure 8*a*), a good longitude for monitoring the northward penetration of the Loop Current into the Gulf of Mexico, has a deltalike distribution with a long negative tail. This distribution implies that the Loop Current growth following an eddy shedding event from a minimum position (within the negative tail of the distribution) toward its mean position is relatively rapid compared to the subsequent growth prior to the eventual shedding of a Loop Current warm-core ring. Figures 8*b*–8*d* are typical of the remaining GSLSE transects in having quasi-normal distributions which pass goodness of fit tests (95% confidence level).

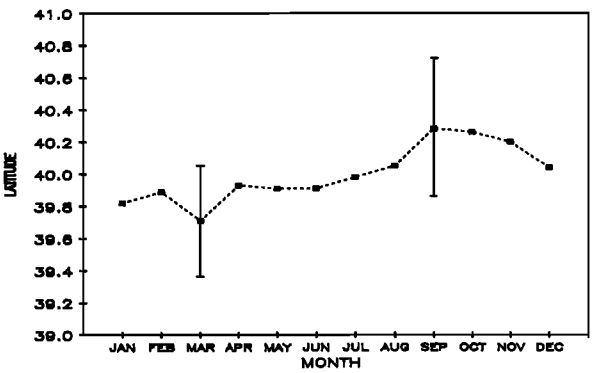

Fig. 7. The 12 monthly Gulf Stream Landward Surface Edge means for the longitude band 70°–44°W. Confidence limits (95%) are drawn for March and September. A one-tail student t test indicates that the March mean is significantly south of the September mean.

4.4. *GSLSE Autocorrelation*

Autocorrelations from the 5-year time series of the GSLSE position for the 45 longitudinal transects between 79.5° and 57.5°W show three separate, distinct e-folding time regimes occurring downstream from 80°W. In order to be totally objective in analyzing the autocorrelations, none of the time series are detrended, although the trend components are larger than the random components in the middle regime near 72°W. Representative autocorrelation plots from the three regimes are illustrated in Figure 9*a*. The e-folding times are estimated from the plotted autocorrelation curves. Figure 9*b*, a plot of the estimated e-folding times, manifests the three regimes which are separated by distinct boundaries near 74°W and 70°W with smooth transitions. Autocorrelation plots within the first regime, the southeastern U.S. coast (79.5°–74.5°W), have a rapid decay with e-folding times of about 1 week which agrees well with those reported by *Bane* [1982] for the small-scale amplitude waves which transit this region. The GSLSE here is dominated by wave processes. The transects in the second regime east of Cape Hatteras from 74.0° to 70.5°W have slowly decaying, flat autocorrelations with long e-folding times. The maximum e-folding time is 10 weeks near 72°W. In the third regime located farther offshore (70.0°–57.5°W) the exponentially decaying autocorrelation curves have e-folding times of the order of 2 weeks. The GSLSE in this regime is dominated by eddy processes.

4.5. *GSLSE Power Spectra*

Smoothed time series (Figures 10*a*–10*c*) and power spectra plots (Figure 10*d*) are given for longitudinal transects 78°W,

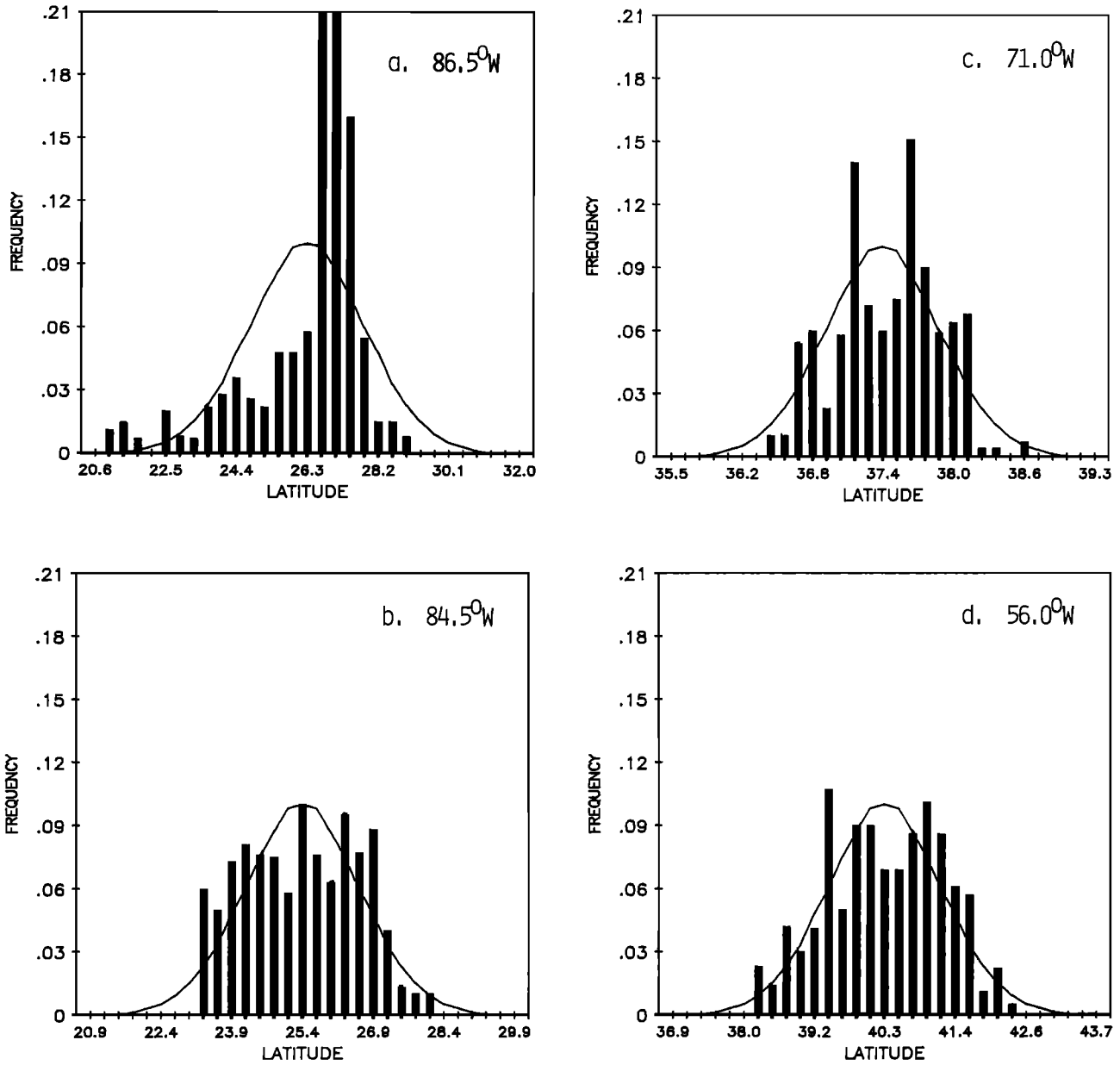

Fig. 8. Probability distribution of Gulf Stream Landward Surface Edge observations for 5 years at four selected longitudinal transects (Figure 8*a*, 86.5°W; Figure 8*b*, 84.5°W; Figure 8*c*, 71.0°W; and Figure 8*d*, 56.0°W). A standard normal curve is provided as a reference. The Gulf Stream Landward Surface Edges have a quasi-normal distributions according to goodness of fit tests, except at 86.5°W (Figure 8*a*). The long negative tail at 86.5°W implies that the Loop Current's northward penetration rate is rapid following an eddy shedding event.

72°W, and 61°W. The raw time series is smoothed by using a simple three-point smoother with weights of 0.25, 0.50, and 0.25. The time series plots show the mean GSLSE latitude as the zero reference line. The time series at 78°W is relatively uneventful compared to the time series at 72°W and 61°W which have large variability associated with meander growth and translation and ring absorption episodes. The time series at 61°W also contains sudden meander detachment (GS WCR formation) episodes. In addition, these two time series and most time series east of 74°W show a long-period trend toward a more northern position. Power spectra are generated from the smoothed time series, which is neither detrended nor prewhitened, using the *IMSL* [1984] software routine FTFREQ. The transform algorithm used to generate the raw spectral estimates is

$$P_i = s^2\pi^{-1} + 2\pi^{-1}\sum_{j=1}^{m-1} \mathrm{ACV}_j(\cos((i-1)j\pi m^{-1})) + \mathrm{ACV}_m\pi^{-1}(\cos((i-1)\pi)) \quad (1)$$

where i is the frequency, s^2 is the variance, ACV is the autocovariance, and m is the number of lags (50). The raw spectral estimates are then smoothed using a Hamming window. The smoothed power spectra are red spectra with the highest ener-

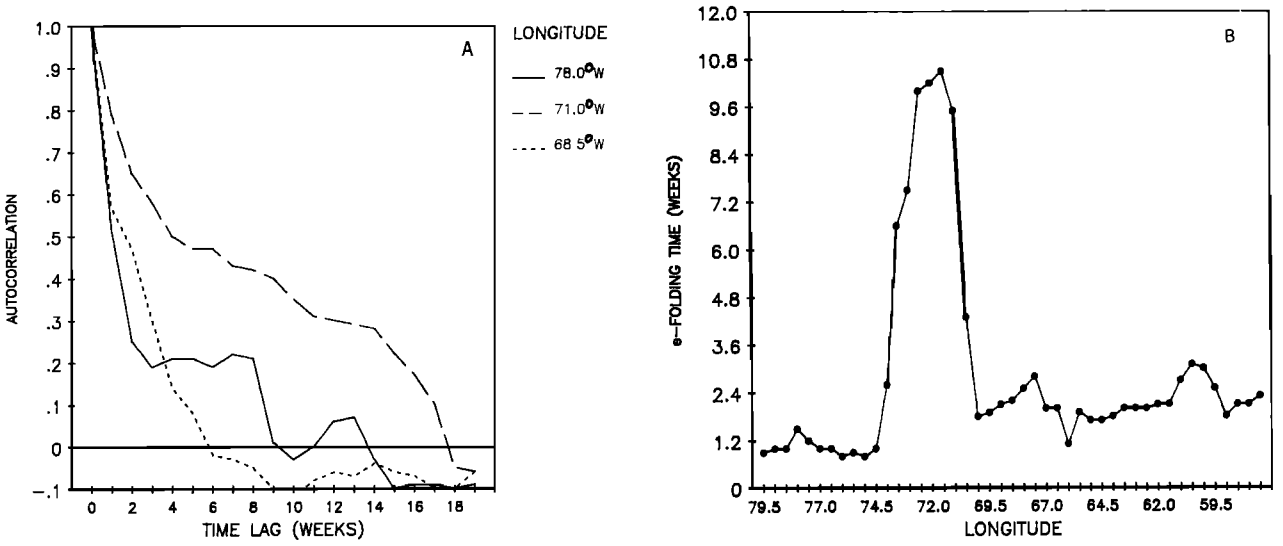

Fig. 9. Normalized Gulf Stream Landward Surface Edge autocorrelation at three selected longitudinal transects (Figure 9*a*) the estimated *e*-folding times for all longitudinal transects between 79.5° and 57.5°W (Figure 9*b*). Three *e*-folding regimes are found for the Gulf Stream along the Carolinas, just offshore of Cape Hatteras, and farther offshore of Cape Hatteras.

gies at the longest periods. The spectra energies apparently decrease to a midperiod plateau between 8 and 20 weeks and thereafter decrease rapidly. The total spectra energies are lowest along the Carolinas (80°–75°W) with the highest local total energies in the Charleston Gyre region (78°–77°W) at periods greater than 1 year. In a relatively small area just downstream from Cape Hatteras (74.5°–73.0°W) the total spectra energies rapidly increase by 2 orders of magnitude with a local peak at 72°W. This region of spectra energy growth has been previously reported by *Watts and Johns* [1982]. Further offshore from Cape Hatteras, the total spectra energies decrease to a local minimum at 69°W, then increase to the maximum observed peak at 61°W, and then decrease slightly to 58°W. The power spectra have good agreement with other published values; for example, the estimates at 78°W (Figure 10*d*) and 73.5°W (not shown) are comparable to the *Olson et al.* [1983, Figure 7*b*] estimates and the *Tracey and Watts* [1986, Figure 8] estimates, respectively.

5. Ring Census

Figure 11 is a spaghetti plot of all the WCR (warm-core ring) and CCR (cold-core ring) tracks observed during the 5-year study period. A total of 136 different WCRs and 175 CCRs are observed during the period. The WCRs can be separated into 21 LC WCRs (Loop Current WCRs) and 115 GS WCRs (Gulf Stream WCRs). The LC WCRs generally translate west-southwestward into the western basin of the Gulf of Mexico. The GS WCRs tend to translate west or southwestward between the mean GSLSE and the continental shelf. The CCRs translate west to southwest in the Sargasso Sea south of the stream. An open swath of space separates the GS WCRs from the CCRs. The 5-year mean GSLSE position is located along the northern edge of this open swath being located closer to the GS WCR tracks. The GS WCRs translate closer to the mean GSLSE as a result of the confining effect of the continental shelf. Only four of 67 GS WCRs are observed to have formed south of the mean GSLSE while none of the CCRs are observed to have formed north of the mean GSLSE.

Table 3 is a stratified ring census of the three ring types. In Table 3, column two contains the number of rings observed, column three contains the number of synoptic (weekly) ring observations, and columns four–seven stratify the number of rings by the significant ring events observed (formation and/or absorption). A few significant events occur before or after the 5-year period. The GS WCRs are relatively well chronicled in terms of formation and absorption events. Only about half of the LC WCRs could be identified with a Loop Current eddy shedding event; these are listed under the best category in Table 3, and these shall be used in the rest of the paper to define the characteristics of the LC WCRs. The total number of LC WCRs is much less than the GS WCRs. In comparison to the warm-core rings, few CCR formation or absorption events are observed. Also, the average number of observations per individual CCR is small. The three following sections will discuss the ring types in more detail.

6. Gulf Stream Warm-Core Rings

Table 4 gives the gross statistics for the 115 GS WCRs observed between 75° and 44°W over the 5-year study period. The (scalar) speed and the u and v velocity components are determined from the weekly (or longer) observed ring center position movements. The age, (observed/initial) diameter ratio (weekly observed diameter relative to the initial ring diameter at formation), and surface diameter decay rate are determined from the life histories of 71 GS WCRs whose formations were observed. The mean GS WCR is 17 weeks old (not shown), has an average diameter of 130 km (0.85 the length of its formation diameter), and moves west-southwestward at 2.4 km/d. The presence of the relatively small number of GS WCR observations east of 50°W has a negligible effect on the calculated values given in Table 4. The GS WCR average diameter of 130 km is between the 100-km estimate by *Lai and Richardson* [1977] and the 170-km estimate of *Zheng et al.* [1984]. The GS WCR mean speed of 7 km/d contrasts with

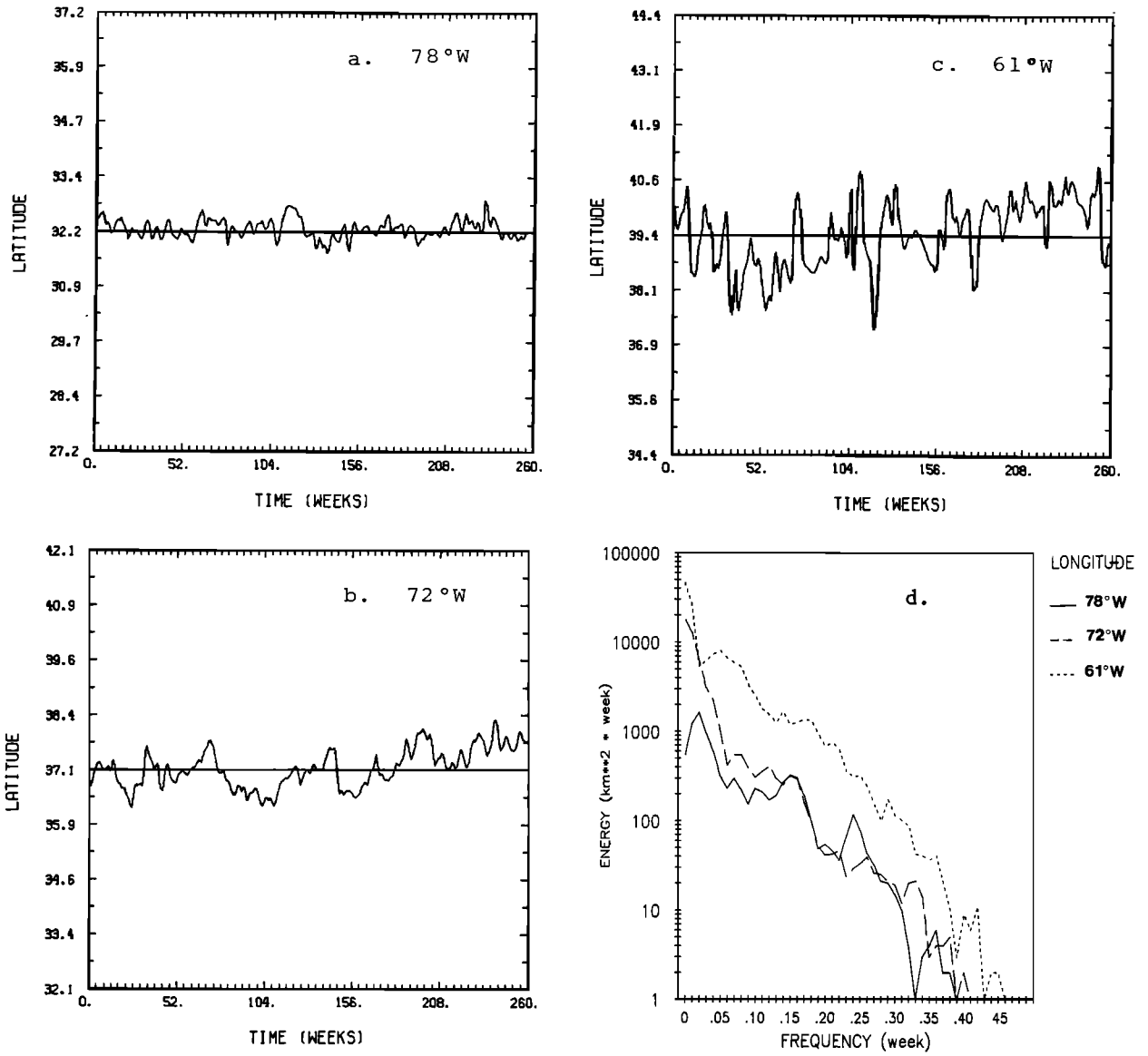

Fig. 10. Smoothed 5-year time series (Figures 10*a*, 10*b*, and 10*c*) and power spectra (Figure 10*d*) of the Gulf Stream Landward Surface Edge at three longitudinal transects. The time series at 78°W is relatively uneventful compared to the others which have large variability associated with meander growth and ring formation/absorption episodes. The power spectra are red with dominant periods of about 1 year. The total spectra energy increases downstream.

the mean velocity of 2.4 km/d west-southwest and the average translation speed (distance between ring formation location and absorption location divided by ring lifetime) of 2.7 km/d (see Table 9) illustrating the complexity of the ring movements. The GS WCR mean speed is slightly higher than the average value of 5–6 km/d found by various other surveys [*Brown et al.*, 1986; *Zheng et al.*, 1984; *Lai and Richardson*, 1977; *Halliwell and Mooers*, 1979]. The maximum observed GS WCR speed of 37 km/d is less than the maximum of 65 km/d reported by *Richardson* [1980*b*] for some rings attached to the Gulf Stream.

A sample of 71 GS WCR life histories has a normalized surface diameter decay rate of −0.026 per week between the weeks of formation and absorption with a 0.34 correlation with ring age. The rate of surface diameter decay is much larger during the first 10 weeks at −0.147 per week. This data sample contains a few cases of GS WCR interactions with the Gulf Stream or other GS WCRs where the surface diameter suddenly decreases or increases (note maximum surface diameter ratio of 1.80 in Table 4). The effect of these cases on the calculated diameter decay rate is small, as they seem to negate one another. *Brown et al.* [1986] also found ring diameter decay in which the average GS WCR semimajor axis length decreases from 75 km at formation to 35 km at absorption with an *e*-folding time of 213 days for rings not interacting with the stream. However, *Zheng et al.* [1984] with a smaller sample of three GS WCRs with 20–60 days of observation finds an opposing growth rate where the GS WCR surface area monotonically increases at a mean rate of 0.013 per day.

The calculated yearly and seasonal mean GS WCR speeds (not shown) are not significantly different.

Table 5 stratifies the GS WCR gross statistics into 2.5°

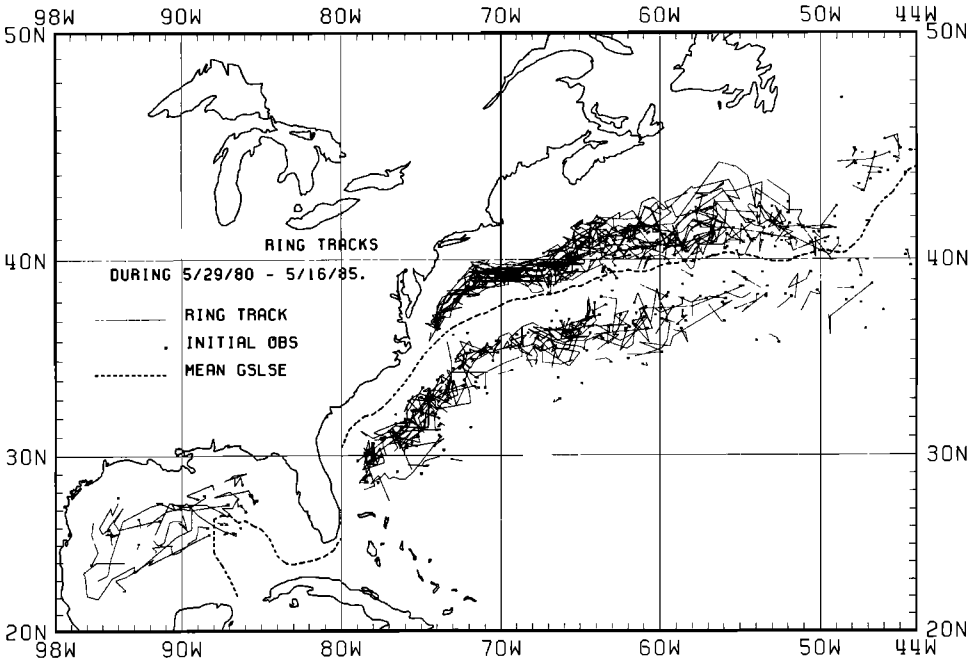

Fig. 11. Observed warm-core and cold-core ring tracks for 5 years. The dashed line is the 5-year mean Gulf Stream Landward Surface Edge.

longitudinal strips from 45° to 75°W. The GS WCR mean ages linearly increase westward (by longitudinal strip) with a 0.38 correlation. The GS WCR average diameter significantly and steadily decreases (133–88 km) west of 65°W. Likewise, the mean (observed/initial) diameter ratios also decrease westward over this area. The GS WCRs located in the Newfoundland Basin (47.5°–45.0°W) are slightly smaller than the GS WCRs just to the west. Geographical departures from the mean GS WCR velocity of 2.4 km/d west-southwest are noted by the mean velocity increase (4–6 km/d) west of 67.5°W and the northward directional shift at 55.1°–57.5°W. The GS WCR mean velocity increases west of 67°W are a result of less scatter (in direction) in the GS WCR movements and not to a spatial increase in the GS WCR speeds, as no significant geographical differences are found for the GS WCR mean speeds.

Table 6 longitudinally stratifies the GS WCR census by 2.5° longitudinal strips. The area of highest GS WCR activity is 65.0°–62.6°W with the largest number of observed GS WCR formations. This is the New England Seamount area where *Fuglister and Worthington* [1951] and *Fuglister* [1963] noted the frequent occurrence of large meanders and ring formation. The GS WCR absorption events listed in Table 6 are split into absorption by the Gulf Stream and by another GS WCR. The largest number of GS WCR absorptions (by the Gulf Stream) occurs 75.0°–72.6°W with a second maximum 60.0°–57.6°W. No GS WCR formations are observed west of 70°W. A minimum absorption area exists at 72.5°–67.6°W. This region is a

TABLE 3. A 5-Year Ring Census of Gulf Stream Warm-Core Rings (GS WCR), Loop Current Warm-Core Rings (LC WCR, best set used for this study), and Cold-Core Rings (CCR)

	Number of Rings	Total Number Observations	F and A	F Only	A Only	Neither F nor A
GS WCR	115	1020	66	5	13	31
LC WCR	21	164	7	2	1	11
(best)	(13)	(123)	(7)	(2)	(1)	(3)
CCR	175	707	7	19	7	142

F is the ring formation observed and A is the ring absorption observed.

TABLE 4. The 5-Year Gross Statistics for 115 Gulf Stream Warm-Core Rings (GS WCR), 13 Loop Current Warm-Core Rings (LC WCR), and 175 Cold-Core Rings (CCR)

	Number	Mean	S.D.	Minimum	Maximum
		Scalar Speed, km/d			
GS WCR	905	6.8	4.9	0	37
LC WCR	108	6.2	4.5	0	28
CCR	539	7.2	4.8	0	28
		U Velocity Component, km/d			
GS WCR	905	−2.3	6.1	−37	26
LC WCR	108	−2.3	5.7	−26	14
CCR	539	−0.6	6.3	−21	23
		V Velocity Component, km/d			
GS WCR	905	−0.5	5.2	−27	24
LC WCR	108	−0.7	4.6	−17	11
CCR	539	−0.7	5.9	−14	27
		Surface Diameter, km			
GS WCR	1015	129	42.7	46	370
LC WCR	107	222	69.1	102	389
CCR	707	105	28.0	35	230
		(Observed/Initial) Surface Diameter Ratio			
GS WCR	838	0.85	0.30	0.20	1.80
		Surface Diameter Decay Rate			
GS WCR	832	−0.026 per week			
LC WCR	86	−0.024 per week			

TABLE 5. Longitudinally Stratified Gulf Stream Warm-Core Ring Statistics

Longitudinal Strip Limits	Mean Diameter		Mean Speed		Mean Velocity		Mean Age, week	Mean O/ID ratio
	km	Number	km/d	Number	km/d	Direction		
75.0°–72.6°W	88	(69)	8.2	(69)	5.7	224°	31	0.6
72.5°–70.1°W	103	(111)	6.7	(111)	4.1	251°	25	0.7
70.0°–67.6°W	119	(83)	7.0	(79)	4.6	270°	19	0.8
67.5°–65.1°W	133	(159)	6.7	(151)	2.0	244°	15	0.8
65.0°–62.6°W	143	(148)	6.3	(133)	2.0	261°	14	0.9
62.5°–60.1°W	137	(112)	7.0	(102)	1.9	292°	14	0.9
60.0°–57.6°W	140	(85)	7.0	(74)	2.5	241°	14	1.0
57.5°–55.1°W	139	(80)	7.0	(68)	1.4	014°	10	1.0
55.0°–52.6°W	133	(69)	6.3	(59)	2.1	301°	11	0.9
52.5°–50.1°W	144	(43)	7.2	(32)	1.4	289°	8	0.9
50.0°–47.6°W	139	(32)	5.9	(18)	1.7	212°	6	1.0
47.5°–45.1°W	119	(20)	6.8	(9)	2.3	221°	2	1.0

(O/ID stands for observed/initial diameter).

GS WCR transit zone with few formations or absorptions. It is well known that GS WCRs are reabsorbed by the Gulf Stream; however, they can also be absorbed by other GS WCRs as occurred in 14 of the 79 (18%) cases. These events are observed within the region 67.5°–55°W with nearly half occurring between 67.5°–65.0°W. No case of a GS WCR formation by the splitting up of a GS WCR is observed. Also, no case of a GS WCR dissipation within the slope water region is observed, although such an occurrence cannot be ruled out. Thus it appears that GS WCRs are eventually reabsorbed by the Gulf Stream (notwithstanding the possibility of being absorbed by another GS WCR which is later reabsorbed by the stream).

Table 7 gives the yearly tallies of GS WCR formation and absorption or first observation and last observation. Apparently, 22 GS WCRs are formed and absorbed per year with some interannual variability. *Lai and Richardson* [1977] estimate that five GS WCRs form over a smaller region (about 55°–75°W). This study estimates 11 GS WCRs for the same region, a difference possibly due to the different sampling periods and the interannual change in ring production. Figures 12 and 13 show the GS WCR formation or first observation and absorption or last observation locations of 115 GS WCRs (some of the events occurred outside the 5-year period). The spatial distribution of the GS WCR formation or first observation locations is fairly uniform from 65° to 45°W with fewer between 70° and 65°W and none west of 70°W. The spatial frequency of the GS WCR absorption or last observation locations appears uniform over the entire slope water region except for a minimum between 71° and 67°W.

A sample of 66 GS WCRs whose formations and absorptions are observed (some of these events occur before or after the 5-year study period) is analyzed to discern the typical GS WCR lifespan pattern. Table 8 matches the 66 GS WCR formations and absorptions for the 2.5° longitudinal strips. All the GS WCRs absorbed west of 67.6°W have long-distance translations. Local translations (GS WCR formation and absorption occur within the same 2.5° longitudinal strip) constitute almost half of the GS WCRs formed between 67.5° and 52.6°W. The GS WCR trends east of 52.5°W are less clear since few lifespans were observed. However, the synoptic record implies that GS WCRs east of 48°W (the Tail of the Grand Banks) have short lifespans.

Figure 14 compares the 66 known GS WCR and seven known LC WCR lifespans (some overlap the 5-year study period). The distribution of the GS WCR lifespans in this study agrees with the 10-year GS WCR study of *Brown et al.* [1986] (which overlaps the period of this study) in having a

TABLE 6. Longitudinally Stratified 5-Year Gulf Stream Warm-Core Ring (GS WCR) Event Census

Longitudinal Strip Number	Longitudinal Limits	Number Observed	Number Formed	Number Absorbed by Stream	Number Absorbed by GS WCR
1	75.0°–72.6°W	13	0	12	0
2	72.5°–70.1°W	16	0	2	0
3	70.0°–67.6°W	19	3	2	0
4	67.5°–65.1°W	23	5	2	5
5	65.0°–62.6°W	27	16	8	1
6	62.5°–60.1°W	18	8	6	2
7	60.0°–57.6°W	22	11	9	2
8	57.5°–55.1°W	19	9	5	1
9	55.0°–52.6°W	19	6	7	0
10	52.5°–50.1°W	19	5	2	0
11	50.0°–47.6°W	15	2	4	0
12	47.5°–45.1°W	13	1	1	0
Total			66	60	11

TABLE 7. Gulf Stream Warm-Core Ring Yearly Event Census

	Year				
	1	2	3	4	5
Number formed	14	11	11	16	14
Number first observed	12	6	10	8	8
Total	26	17	21	24	22
Number absorbed	17	10	14	15	15
Number last observed	9	6	9	6	8
Total	26	16	23	21	23

bimodal distribution, a mean of 19 weeks (133 days compared to 130 days), and the occurrence of the frequency minimum which splits the bimodal distribution at the mean frequency. Most GS WCR lifespans are less than 13 weeks. The highest frequency of GS WCR lifespans occurs from 1 to 4 weeks with a secondary frequency peak at 23–28 weeks. This study's maximum lifespan of 64 weeks (448 days) is longer than the 399 day lifespan of Brown et al. Table 9 compares the mean and maximum lifespans and translations of the known GS WCRs and LC WCRs. The mean and maximum lifespans for both types are similar, 18 weeks and 62 weeks, respectively. The mean translation (distance from formation location to absorption location) is not significantly different between the GS WCRs and the LC WCRs. Thus both types of warm-core rings appear to have similar lifespans and translations.

The distribution of the translations of the 66 known GS WCRs (Figure 15) is biased toward the southwest and west as expected due to the topographic constraints which force the long-term drift in that direction. The short translations (<200 km) are split evenly between northward and southward components. The longest GS WCR translation is 1255 km to the west-southwest. By comparison the longest LC WCR translation is 911 km to the west-southwest. The mean vector translation of the GS WCRs is almost twice that of the LC WCRs (Table 9).

Figure 16, a frequency distribution of the initial (formation) diameters of 71 GS WCRs and 9 LC WCRs, shows that the GS WCRs have smaller initial diameters (mean of 165 km compared to 275 km) than the LC WCRs.

7. Loop Current Warm-Core Rings

In the Gulf of Mexico, 13 warm-core features can be identified by a known or probable Loop Current shedding event during the 5-year period. The nearly complete lack of summertime satellite observations in the Gulf of Mexico hinders the tracking of LC WCRs into the western basin of the Gulf of Mexico (and ultimately to their dissipation). Fortunately, some drifting buoy observations are available to track some of these LC WCRs. The nine warm-core features initially observed in the western basin are not included in this study, although some of these may, in fact, have been aging LC WCRs.

Because the observations in the western Gulf are temporally sporadic, no conclusion from this study can be made on the existence of a persistent anticyclonic gyre as reported by *Cochran* [1972].

Table 4 gives the LC WCR statistics. The LC WCRs are nearly twice the size of the GS WCRs (223–129 km) and have the same velocity (2.4 km/d west-southwest). The LC WCR mean speed of 6.2 km/d is close to the 4–6 km/d for one LC WCR estimated by *Cochran* [1972] but is more than the 3 km/d for six LC WCRs calculated by *Elliott* [1982]. A sample of eight LC WCRs, whose formations are observed, has a normalized surface diameter decay rate of −0.024 per week which compares favorably with the −0.026 rate for the GS WCRs.

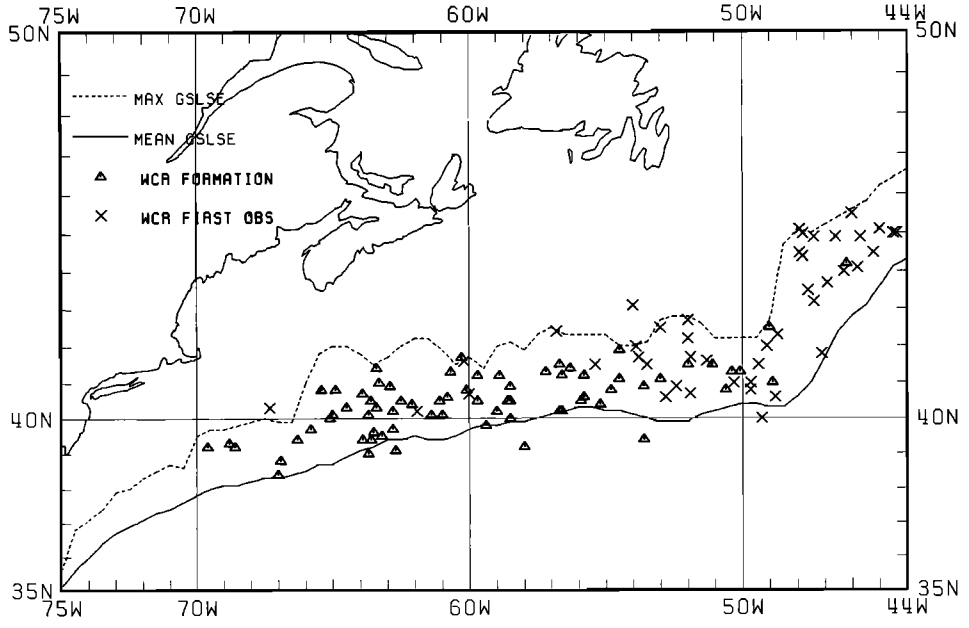

Fig. 12. Formation or first observation locations of 115 Gulf Stream warm-core rings. Triangles demark observed formations while crosses demark first sightings. The solid line is the mean, and the dashed line is the extreme Gulf Stream Landward Surface Edge. The spatial distribution appears uniform from 65° to 45°W.

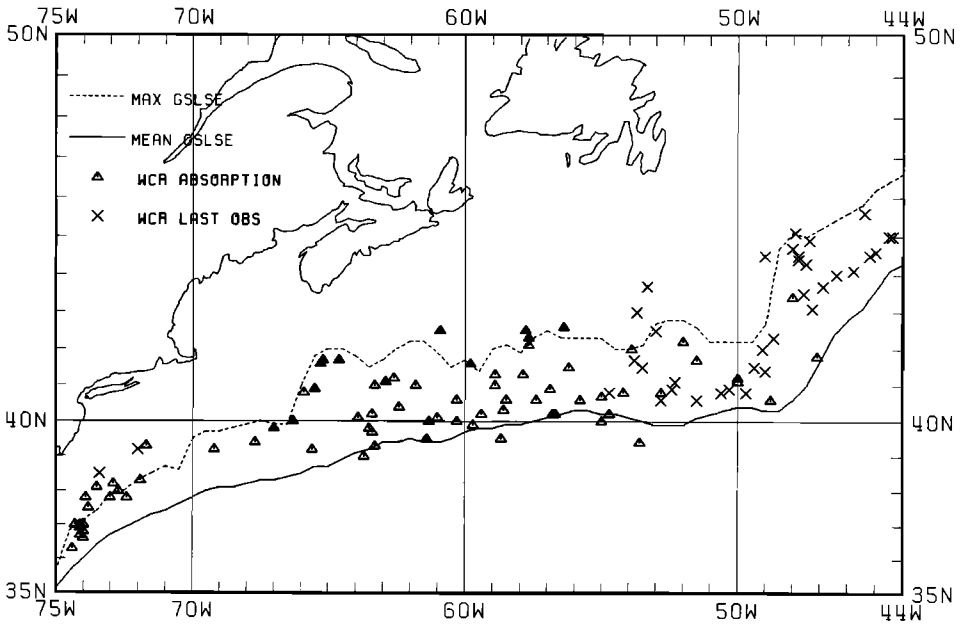

Fig. 13. Observed center positions of last observation or prior to absorption for 115 Gulf Stream warm-core rings. Open triangles demark observed absorptions and crosses demark last sightings. The solid triangles indicate a ring absorption by another warm-core ring. The solid and dashed lines are the 5-year mean and extreme Gulf Stream Landward Surface Edge positions. A warm-core ring absorption frequency minimum exists between 71° and 67°W.

Figure 17 gives time lines for the 13 LC WCRs. These are categorized by size into major and minor LC WCRs. The terms major warm gyre and minor warm gyre have been used by *Vukovich et al.* [1979]. Major LC WCRs are formed when most of the Loop Current penetration pinches off. Minor LC WCRs are formed when a small protrusion, usually a northern lobe, of the loop pinches off.

Roughly, eight major LC WCR shedding events occurred during the 5-year study period (Figure 17); three of these were quickly reabsorbed by the Loop Current (lifespans less than 1 month), and the other five drifted into the western Gulf of Mexico. The mean temporal gap between the formations of the four known major LC WCRs which drifted into the western basin of the Gulf of Mexico is 12 months with a variability of 6–16 months. This supports *Elliott*'s [1982] estimate that a mean yearly advection is required to balance the salt budget of the western basin.

TABLE 8. Matching of Gulf Stream Warm-Core Ring Formation and Absorption Longitudinal Strips (Strip Limits Given in Table 6)

Formation Strip Number	Absorption Strip Number												
	1	2	3	4	5	6	7	8	9	10	11	12	Total
1													0
2													0
3	2	1											3
4	2	1	0	2	1								6
5	5	3	1	3	5								17
6	3	0	0	1	1	3							8
7			1	0	0	3	7						11
8					1	1	2	5	1				10
9					0	1	1	1	3				6
10					1	0	1	0	0	1	1		4
11							1						1
12													0
Total	12	5	2	6	9	8	12	6	4	1	1	0	66

The temporal gap between the seven known major LC WCR shedding events is 8.5 months with a variability of 4–16 months which is similar to the *Behringer et al.* [1977] findings. The major LC WCR shedding events show no seasonal bias, having formed in months December, January, February, April, May, and June. In contrast, Behringer found an early summer bias.

Two major LC WCR dissipations in the western Gulf of Mexico are estimated from drifting data buoy reports. These LC WCRs had lifespans of 40 and 59 weeks, yielding an average lifespan of about 1 year which agrees with Elliott's lifespan found for one WCR.

The average major LC WCR formation center point is near 26°N 87°W with an average initial diameter of 307 km. This is smaller than the average diameter of 400 km reported for three major LC WCRs by *Vukovich et al.* [1979], who also noted that the eddies tend to be elliptical in shape. The average size of the observed major LC WCRs is 250 km with a maximum size of 390 km. *Elliott* [1982], using the historical data set of 1965–1972, finds a mean diameter (measured by the curvature of the 20°C isotherm) of 366 km for 15 (apparently major) LC WCR observations in the eastern Gulf of Mexico with a maximum diameter of 488 km. The difference in mean sizes is probably attributable to the measurement methods.

At least five minor LC WCR shedding events occurred in slightly more than 5 years. Of these, three were apparently reabsorbed by the Loop Current, one translated into the western basin, and one fate is unknown. Two minor LC WCR formation events are observed near 28°N 86°W with an average initial LC WCR diameter of 185 km. The average diameter of the minor LC WCRs is 165 km with a minimum observed diameter of 100 km. The average mean speeds of the major and minor LC WCRs are similar at 6 km/d. The

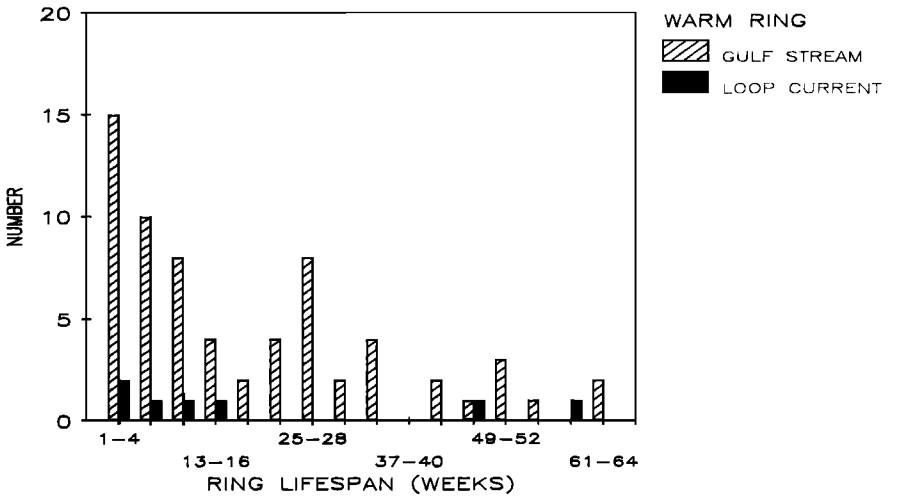

Fig. 14. Known lifespans of 66 Gulf Stream warm-core rings and seven Loop Current warm-core rings.

average lifetime of the two known minor LC WCRs is 2.5 months which is shorter than the major LC WCRs, but this value is unreliable given the small sample size and the unknown lifespan of the minor LC WCR which drifted into the western basin.

8. Cold-Core Rings

CCRs are more difficult to delineate in satellite imagery by surface thermal signal than the warm-core rings since the CCR surface gradient boundary tends to be weaker and the denser cold water core tends to sink with time, wiping out the SST anomaly. CCRs are best discerned during springtime when the SST gradients are greater (345 of 707 CCR observations observed in spring) and when interacting with the Gulf Stream which produces a hooklike entrainment pattern of warmer water around the CCR. The CCR identification problems prevent the making of good estimates of both the number of CCRs and the average CCR lifespan from the satellite-derived data smaples.

The study observed about 175 CCR-type features over the 5-year period. The apparent yearly average of 35 CCRs is much higher than *Fuglister*'s [1972] estimate of 5–8 per year. However, *Fofonoff* [1981] estimated that the Gulf Stream's flux of mass and energy (from kinetic energy to potential energy) could propagate a maximum of 50 rings (both GS WCR and CCR) of 100-km radius yearly. The Fofonoff 5000 km^2 total annual ring surface area is greater than this study's 3400 km^2 area (57 CCRs and GS WCRs of 60-km mean radius). Thus 35 CCRs yearly is not improbable if the southward recirculation is largely CCR driven. However, there is much uncertainty in this study's CCR number. For instance, multiple observations during different time segments of the same CCR life history may have been inadvertently counted as separate CCRs. One indicator of this is that few CCRs are tracked southeastward of 34°N 70°W from a formation (or first observation) east of Cape Hatteras as *Richardson* [1980*b*] and *Lai and Richardson* [1977] observed, although many CCR trackings are observed in both regions (Figure 11). Alas, the author suggests that about 20 CCRs are propagated early, about the same number as the GS WCRs.

Because the CCR life histories are uncertain, only general information (Figure 4) can be gleaned from the 707 CCR ob-

TABLE 9. Lifespan and Translation Comparisons of Gulf Stream Warm-Core Rings (GS WCR) and Loop Current Warm-Core Rings (LC WCR)

	GS WCR	LC WCR
Number	66	7
Mean lifespan, weeks	19	18
Maximum lifespan, weeks	64	60
Mean translation, km	359	270
Maximum translation	1255 km at 247°T	911 km at 251°T
Mean vector translation	315 km at 256°T	161 km at 251°T

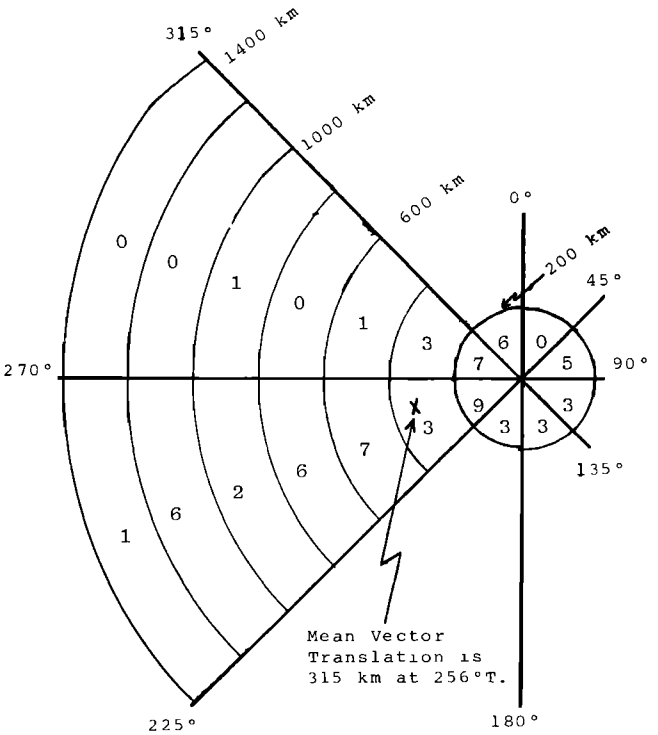

Fig. 15. Frequency distribution of the translations of 66 Gulf Stream warm-core rings.

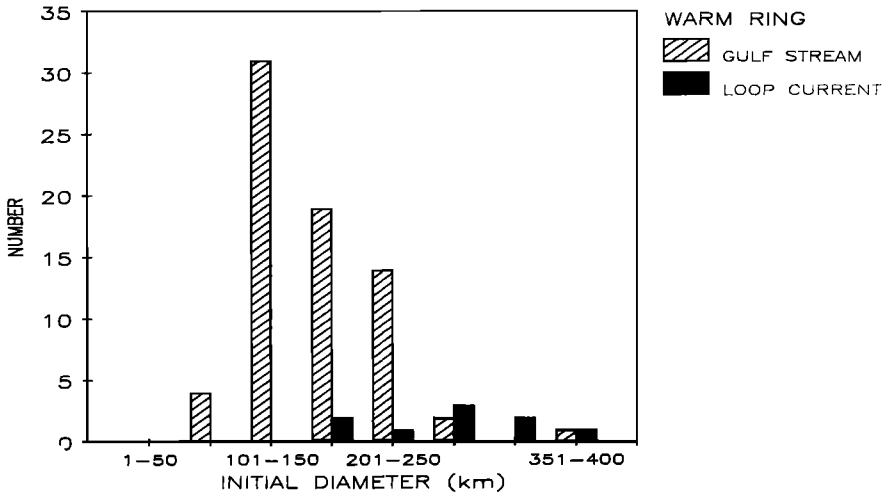

Fig. 16. The initial (formation) diameters of 71 Gulf Stream warm-core rings and nine Loop Current warm-core rings.

servations during the study period. The mean CCR diameter is 105 km which is much smaller than *Lai and Richardson*'s [1977] estimate of 250 km. The discrepancy is largely due to the measurement methods. This study measured the diameter of the cool surface anomaly which does not encompass the rotating remnant of the Gulf Stream meander, whereas, Lai and Richardson measured the 15°C extent at 500 m depth. Since contoured vertical temperature profiles of CCRs are "dome shaped," the horizontal extent of the isotherms expands with depth. The CCR mean speed is 7 km/d. The average CCR velocity is 1 km/d southwestward which is low in comparison to *Richardson*'s [1980*b*] determination of 4 km/d for 12 CCRs measured by drifting buoys. The *Ring Group* [1981] has estimated the mean CCR lifetime to be 1.0–1.5 years.

9. Conclusions

A 5-year data set containing weekly infrared satellite observations of the GSLSE and associated rings is analyzed to determine the gross statistics and the geographical and temporal variability. This data set is unique in having a large geographical span (the Gulf of Mexico and the northwest Atlantic Ocean), a long data period with regular synoptic (weekly) intervals, and a reliable data source (satellite imagery).

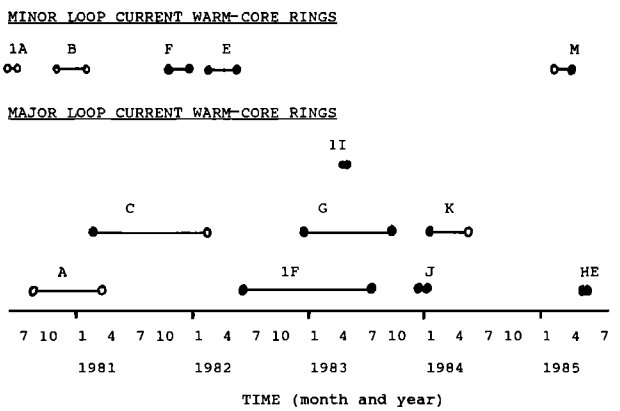

Fig. 17. Time lines for eight major and five minor Loop Current warm-core rings. The solid end points indicate an observed formation/absorption (or dissipation) event.

The 5-year observations in the Gulf of Mexico contain annual gaps from about July–October. These probably have a more adverse affect on understanding the LC WCR movements than they do on understanding the Loop Current variability. The Loop Current has a mean northward penetration to 26.5°N with an extreme intrusion range of 900 km. The northern edge of the loop exhibits some interannual variability resulting from sporadic LC WCR shedding events but little seasonal variability, as the LC WCR shedding events show no seasonal preference. The mean western edge of the loop is near 88.0°W with little evidence of annual or interannual meridional variability. The relative Loop Current northward penetration rate is fast from a minimum position after a WCR shedding event toward its mean position; thereafter, in comparison, the rate is slower over a longer time period until the Loop Current ultimately propagates another major LC WCR. Dynamical model simulations by *Hurlburt and Thompson* [1980] and observations analyzed by *Behringer et al.* [1977] and *Molinari et al.* [1977] indicate that each large loop penetration leads to a LC WCR formation. LC WCR propagation has no clear seasonal preference.

LC WCRs are grouped by spatial scale into major and minor LC WCRs. A major LC WCR is formed, on average, every 8.5 months when most of the Loop Current penetration pinches off (307-km mean initial diameter). Some of these major LC WCRs quickly reabsorb back into the Loop Current while about one per year advects into the western basin of the Gulf of Mexico. Minor LC WCRs are formed when a small northern lobe of the Loop Current pinches off (185-km mean initial diameter). About one minor LC WCR is formed annually. Most minor LC WCRs are apparently reabsorbed back into the Loop Current, although some do translate into the western basin.

The Gulf Stream System variability increases downstream from the Florida Straits to the Grand Banks. The interannual variability (between years) is equal to the annual variability (between seasons) over the longitudinal band 74°–44°W. The GSLSE position downstream past Cape Hatteras (74°–44°W) has slowly, but significantly shifted northward from year 1 to year 5. Beginning just downstream from Cape Hatteras (70°–44°W), the GSLSE annually shifts from a northernmost position in September to a southernmost position in March. The

largest magnitude of this annual shift occurs in the Newfoundland Basin.

Possible topographic effects (by the Charleston Bump, Cape Hatteras, the New England Seamounts, and the Grand Banks) on the GSLSE and (for some) the GS WCRs are evidenced by the following. The mean GSLSE path suddenly shifts at the Charleston Bump and at the Tail of the Grand Banks. The total spectra energies have local maximums just past the Charleston Bump and Cape Hatteras and are largest immediately downstream of the New England Seamounts (spectra energies are not available at the Grand Banks). The highest frequency of GS WCR observations and formations is observed near the New England Seamounts. The GSLSE increases its range and standard deviation just downstream of Cape Hatteras and the Grand Banks.

Frequency distributions of the GSLSE at most longitudinal transects have a quasi-normal distribution according to goodness of fit tests.

Individual 5-year time series of the GSLSE at longitudinal transects 79.5°–57.5°W are analyzed. The GSLSE power spectra are red with dominant energies at periods of 1 year or more. The total spectra energy increases downstream to a maximum detected peak at 61°W. The *e*-folding times of the GSLSE, estimated from the calculated autocorrelations, are split into three well-defined geographical regimes. The GSLSE *e*-folding times are about 1 week along the Carolines, 10 weeks just past Cape Hatteras, and about 2 weeks farther downstream (70–57.5°W).

About 22 GS WCRs are formed and absrobed annually over the region 75°–44°W. The GS WCR events east of 50°W are not well chronicled, but the Newfoundland Basin appears to be an area of dynamic eddy activity. Observations of GS WCR translations westward from the region east of 50°W are infrequent which could be due to the constrainment of the Newfoundland rise and the close proximity of the Labrador Current to the north. The spatial frequency of GS WCR observations is highest in the New England Seamount region (65°–62°W). The spatial frequency of GS WCR formations is highest near the New England Seamounts and evenly distributed east of 60°W. No GS WCR formations are observed west of 70°W. The spatial frequency of GS WCR absorptions is highest near Cape Hatteras, least frequent from 71° to 66°W, and evenly distributed east of 66°W. Although most GS WCRs are absorbed by the Gulf Stream, 18% of the absorption cases are observed to be by other GS WCRs.

The average initial GS WCR diameter after formation is 165 km (compared to 305 km for the major LC WCRs) and has an average diameter decay rate of −0.026 per week (similar to the LC WCRs). The GS WCR mean lifespan is 19 weeks (similar to the LC WCRs), but the most frequent lifespan is 4 weeks or less. The GS WCR mean speed is 7 km/d (similar to the LC WCRs). The GS WCR mean velocity is 2.4 km/d west-southwest (same for the LC WCRs).

A typical GS WCR life history is formation near the New England Seamounts, a velocity of 2.4 km/d west-southwestward, a surface diameter decay with age (decay rate larger during the first 10 weeks), and eventual absorption by the Gulf Stream near Cape Hatteras.

Cold-core ring life histories are tentative, and therefore only general statistics are determined which give a mean cool-core surface diameter of 105 km and a mean velocity of 1 km/d southwestward.

Acknowledgments. The author is grateful for the advice of the anonymous reviewers and the following individuals of the National Meteorological Center: William Gemmill, D. B. Rao, David Feit, Lawrence Burroughs, Paul Julian, and Larry Breaker. The author also salutes the work of Jenifer Clark in analyzing satellite imagery for the Oceanographic Analysis charts. Ocean Products Center Contribution 9.

REFERENCES

Auer, S. J., New daily oceanographic analyses, *gulfstream*, *6*(4), 3–7, 1980.

Auer, S. J., A reversal of the normal Loop Current boundary pattern, *Oceanogr. Mont. Summ.*, *3*(1), 3, 1982.

Auer, S. J., Gulf Stream System landward surface edge statistics, *NOAA Tech. Memo. NWS NMC 67*, 20 pp., 1983.

Baig, S., D. Gaby, and J. Wilder, A provisional Gulf Stream System climatology, *Mar. Weather Log*, *25*(5), 323–347, 1981.

Bane, J. M., Jr., Initial observations of the subsurface structure and short-term variability of the seaward deflection of the Gulf Stream off Charleston, South Carolina, *J. Geophys. Res.*, *88*, 4673–4684, 1982.

Behringer, D., R. Molinari, and J. Festa, The variability of anticyclonic current patterns in the Gulf of Mexico, *J. Geophys. Res.*, *82*, 5469–5476, 1977.

Brown, O. B., P. C. Cornillon, S. R. Emmerson, and H. M. Carle, Gulf Stream warm rings: A statistical study of their behavior, *Deep Sea Res.*, *33*, 1459–1473, 1986.

Cochran, J. D., Separation of an anticyclone and subsequent developments in the Loop Current (1969), in *Contributions on the Physical Oceanography of the Gulf of Mexico, Texas A & M Univ. Oceanogr. Stud.*, vol. 2, Gulf Publishing, Houston, Tex., 1972.

Cornillon, P., The effect of the New England Seamounts on Gulf Stream meandering as observed from satellite IR Imagery, *J. Phys. Oceanogr.*, *16*, 386–389, 1986.

Dietrich, G., K. Kalle, W. Krauss, and G. Siedler, *General Oceanography*, 626 pp., John Wiley, New York, 1975.

Elliott, B. A., Anticyclonic rings in the Gulf of Mexico, *J. Phys. Oceanogr.*, *12*, 1292–1309, 1982.

Fofonoff, N. P., The Gulf Stream System, in *Evolution of Physical Oceanography, Scientific Surveys in Honor of Henry Stommel*, pp. 112–139, MIT Press, Cambridge, Mass., 1981.

Fuglister, F. C., Gulf Stream '60, *Prog. Oceanogr.*, *1*, 265–373, 1963.

Fuglister, F. C., Cyclonic rings formed by the Gulf Stream 1965–1966, in *Studies in oceanography*, vol. 1, edited by A. L. Gordon, 194 pp., Gordon and Breach, New York, 1972.

Fuglister, F. C., and A. D. Voorhis, A new method of tracking the Gulf Stream, *Limnol. Oceanogr.*, *10*, Suppl., R115–124, 1965.

Fuglister, F. C., and L. V. Worthington, Some results of a multiple ship survey of the Gulf Stream, *Tellus*, *3*, 1–14, 1951.

Gemmill, W. H., and S. J. Auer, Operational regional sea surface temperature and ocean feature analyses paper presented at First International Conference on Meteorology and Air/Sea Interaction of the Coastal Zone, American Meteorological Society, The Hague, Netherlands, 1982.

Halliwell, G. R., and C. N. K. Mooers, The space-time structure and variability of shelf water-slope water and gulf stream surface temperature fronts and associated warm-core eddies, *J. Geophys. Res.*, *84*, 7707–7725, 1979.

Halliwell, G. R., and C. N. K. Mooers, Meanders of the Gulf Stream downstream from Cape Hatteras 1975–1978, *J. Phys. Oceanogr.*, *13*, 1275–1292, 1983.

Hansen, D. V., Gulf Stream meanders between Cape Hatteras and the Grand Banks, *Deep Sea Res.*, *17*, 495–511, 1970.

Hansen, D. V., and G. A. Maul, A note on the use of sea surface temperature for observing ocean currents, *Remote Sens. Environ. Sci.*, *1*, 161–164, 1970.

Huh, O. K., W. J. Wiseman, and L. J. Rouse, Intrusion of the Loop Current waters into the west Florida continental shelf, *J. Geophys. Res.*, *86*, 4186–4192, 1981.

Hurlburt, H. E., and J. D. Thompson, A numerical study of Loop Current intrusions and eddy shedding, *J. Phys. Oceanogr.*, *10*, 1611–1651, 1980.

IMSL Inc., User's Manual, *Fortran Subroutines for Mathematics and Statistics*, IMSL Inc., Houston, Tex., 1984.

Iselin, C. O'D, Preliminary report on long-period variations in the

transport of the Gulf Stream system, *Pap. Phys. Oceanogr. Meteorol.*, *8*(1), 1–40, 1940.

Lai, D., and P. L. Richardson, Distribution and movement of Gulf Stream rings, *J. Phys. Oceanogr.*, *7*, 670–683, 1977.

Legeckis, R., Satellite observations of the influence of bottom topography on the seaward deflection of the Gulf Stream off Charleston, South Carolina, *J. Phys. Oceanogr.*, *9*, 483–497, 1979.

Leipper, D. F., A sequence of current patterns in the Gulf of Mexico, *J. Geophys. Res.*, *75*, 637–657, 1970.

McClain, E. P., W. G. Pichel, and C. C. Walton, Comparative performance of AVHRR-based multichannel sea surface temperatures, *J. Geophys. Res.*, *90*, 1587–1601, 1985.

Molinari, R. L., S. Baig, D. W. Behringer, G. A. Maul, and R. Legeckis, Winter intrusions of the Loop Current, *Science*, *198*, 505–507, 1977.

Niiler, P. P., and W. S. Richardson, Seasonal variability of the Florida Current, *J. Mar. Res.*, *31*, 144–167, 1973.

Nof, D., On the response of ocean currents to atmospheric cooling, *Tellus*, *35A*, 60–72, 1983.

Nowlin, W. D., Jr., Winter circulation patterns and property distributions, in *Contributions on the Physical Oceanography of the Gulf of Mexico*, vol. 2, edited by L. Capurro and J. L. Reid, pp. 3–51, Gulf Publishing Co., Houston, Tex., 1972.

Olson, D. B., O. B. Brown, and S. R. Emmerson, Gulf Stream frontal statistics from Florida Straits to Cape Hatteras derived from satellite and historical data, *J. Geophys. Res.*, *88*, 4569–4577, 1983.

Richardson, P. L., Benjamin Franklin and Timothy Folger's first printed chart of the Gulf Stream, *Science*, *207*, 643–645, 1980*a*.

Richardson, P. L., Gulf Stream ring trajectories, *J. Phys. Oceanogr.*, *10*, 90–104, 1980*b*.

Richardson, P. L., Gulf Stream trajectories measured with free-drifting buoys, *J. Phys. Oceanogr.*, *11*, 999–1010, 1981.

Ring Group, Gulf Stream cold-core rings: Their physics, chemistry, and biology, *Science*, *212*, 1091–1100, 1981.

Robinson, A. R., J. R. Luyten, and F. C. Fuglister, Transient Gulf Stream meandering, 1, An observational experiment, *J. Phys. Oceanogr.*, *4*, 237–255, 1974.

Robinson, M. K., R. A. Bauer, and E. H. Schroeder, Atlas of North Atlantic—Indian Ocean monthly mean temperatures and mean salinities of the surface layer, *U.S. Nav. Oceanogr. Off. Ref. Publ.*, *18*, 1979.

Stommel, H., *The Gulf Stream, A physical and dynamical description*, University of California Press, Berkley, 1960.

Sturges, W., and J. C. Evans, On the variability of the Loop Current in the Gulf of Mexico, *J. Mar. Res.*, *41*, 639–653, 1983.

Tracey, K. L., and D. R. Watts, On Gulf Stream meander characteristics near Cape Hatteras, *J. Geophys. Res.*, *91*, 7587–7602, 1986.

Vazquez, J., and D. Watts, Observations on the propagation and growth, and predictability of Gulf Stream meanders, *J. Geophys. Res.*, *90*, 7143–7151, 1985.

Vukovich, F., B. Crissman, M. Bushnell, and W. King, Some aspects of the oceanography of the Gulf of Mexico using satellite and in situ data, *J. Geophys. Res.*, *84*, 7749–7768, 1979.

Watts, D. R., and W. E. Johns, Gulf Stream meanders: Observations on propagation and growth, *J. Geophys. Res.*, *87*, 9467–9476, 1982.

Webster, F., A description of Gulf Stream meanders off Onslow Bay, *Deep Sea Res.*, *9*, 130–143, 1961.

Worthington, L. V., On the North Atlantic circulation, *Johns Hopkins Oceanogr. Stud.*, *6*, 110 pp., 1976.

Worthington, L. V., and H. Kawai, Comparison between deep sections across the Kuroshio and the Florida Current and Gulf Stream, in *Kuroshio, its Physical Aspects*, edited by H. Stommel and K. Yoshida, pp. 371–385, University of Tokyo Press, Tokyo, 1972.

Zheng, Q., V. Klemas, and N. E. Haung, Dynamics of the slope water off New England and its influence on the Gulf Stream as inferred from satellite IR data, *Remote Sens. Environ. Sci.*, *15*, 135–153, 1984.

S. J. Auer, National Environmental Satellite, Data, and Information Service, Suitland, MD 20233.

(Received February 4, 1987;
accepted March 2, 1987.)